Combined time-resolved SAXS and X-ray Spectroscopy methods

2010 J. Phys.: Conf. Ser. 247 012047

(http://iopscience.iop.org/1742-6596/247/1/012047)

Combined time-resolved SAXS and X-ray Spectroscopy methods

Wim Bras, Sergey Nikitenko, Giuseppe Portale, Andy Beale, Ad van der Eerden, Dirk Detollenaere

Netherlands Organisation for Scientific Research (NWO)

DUBBLE@ESRF, BP220, F38043 Grenoble Cedex, France

Utrecht University

Inorganic Chemistry and Catalysis, Utrecht University, Sorbonnelaan 16, 3584 CA Utrecht, The Netherlands

Wim.Bras@esrf.fr

Abstract. Recently developed equipment suitable for quasi simultaneous data collection of SAXS/WAXS and X-ray spectroscopy is discussed. The main applications for this technique are foreseen to be time-resolved studies in inorganic materials relevant for catalysis research and ceramics. The equipment is described and experimental limitations are discussed. Experiments on nanoparticle synthesis and the formation of inorganic materials for catalysis are used as examples of the usefulness of the developed equipment.

1. Introduction

At synchrotron radiation laboratories the combination of several experimental techniques in a single experiment using time-resolved X-ray scattering experiments has become wide spread in the last decade. The synergy between the different data sets that can be obtained is clear in cases where faster time resolution is required, where sample inhomogeneity occurs or where different sample environments are not guaranteed to reproduce the same conditions in independent experiments. The latter can be the case when for instance high temperature furnaces with different X-ray windows are used.

The earliest combinations of SAXS with other techniques can be traced to the use of Differential Scanning Calorimetry(1) and with Wide Angle Scattering (WAXS)(2, 3). The latter is an obvious combination since it is technologically relatively simple to implement and it allows the length scales over which structures can be studied to extend from the conventional SAXS regime to inter atomic distances. Both the combinations of SAXS and WAXS as well as DSC are so wide spread to the extent that most of the recently designed X-ray scattering beam lines are constructed as SAXS/WAXS beam lines. Later combinations with light scattering and birefringence(4) managed to extend the accessible

length scale range to the micrometer range. However, the latter set-up is rather complicated and at present has found only limited applications.

Combinations with spectroscopic techniques like Raman scattering, UV-Vis, Fourier Transform Infra Red spectroscopy and dielectric spectroscopy have also been successfully implemented (5-10). These techniques provide chemical information which is not accessible with X-ray scattering techniques. However, these experimental schemes again have not found a wide spread use yet. Especially for Raman scattering where modern fibre optics make it relatively easy to engineer a combined set-up it is puzzling to see that there are relatively few studies. It is possible that the relative high price of this type of equipment plays a role in this but it is more likely that still many potential users are not aware of the possibilities.

Even though there are in some cases clear advantages in combining techniques it is almost inevitable that in such experiments the data quality of at least one of the techniques will be compromised to some extent. For the earlier generation of SAXS/WAXS beam lines where the divergence of the X-ray beam was still relatively high one had to be aware that the over- and under-focus of the X-ray beam on the two detectors could influence the data adversely. For the third generation SR sources, with their much lower divergences, this is much less of an issue since effectively the 'focal depth of field' is larger than the distance separating the SAXS and WAXS detector. However, there are many other pitfalls. The combination of techniques for combinations sake is something that should be avoided.

Also care has to be taken in the interpretation of the different data sets with respect to the sensitivity of the techniques to certain events. A fine example of this is the debate that ranged for some time early this century in the polymer crystallisation literature. Here the issue was that depending on the simultaneous or time-staggered occurrence of a scattering signal in the SAXS data or the earliest moment of detection of diffraction peaks in the WAXS regime, in a sample that was quenched below the crystallisation temperature, one would be able to distinguish between a crystallisation model that could be described by a spinodal decomposition like mechanism or by a more accepted nucleation and growth mechanism(11-14). Obviously it is much more difficult to prove that something is not there then to prove that a diffraction peak is present. However, since in the SAXS data one used the invariant, and therefore could utilise all the pixels of the SAXS detector, in the WAXS data the relevant diffraction peaks were only mapped upon a limited number of detector pixels. This led to a huge difference in data quality between the two techniques. Besides that, effects like Scherrer broadening due to small crystallite size and thermal broadening due to the elevated temperatures that were required also played a role. Effectively one required a much better WAXS detector than SAXS detector to be able to obtain the same data quality (15). In hindsight one can safely say that the outcome of many experiments was influenced more by the detector quality than by the crystallisation behaviour of the polymers under investigation. In this context it is maybe also worthwhile to observe that a relative large number of crystallisation studies on inorganic materials find the presence of an amorphous precursor before the nano-particles become nano-crystallites. This can be the case but it also is feasible that one deals with disordered nanocrystals which generate diffraction peaks below the detection threshold (16). In the specific case of the crystallisation of semicrystalline polymers it appears that the most wide spread opinion at present is that there indeed is a mesophase observed before the crystallisation starts but there still exists difference of opinion about what exactly this mesophase is. However, from an experimental point of view it is impossible to access the real onset of crystallisation via WAXS since this technique is intrinsically not sensitive enough to measure non-perfect nanocrystals at elevated temperatures (15). The SAXS/WAXS data clearly has to be complemented with data from other experimental techniques and modelling before the ultimate answer will be found.

In the domain of X-ray based techniques the cases where scattering and diffraction might not provide all the answers one can in the first place try to utilise 'total scattering' methods (17, 18) which can provide information about the order inside the nanoparticles but in other cases one can revert to the spectroscopic techniques that have been mentioned above. Another technique that can generate data relevant for the earliest stages of a crystallisation process or that can shine light on the structure of small disordered domains is X-Ray Absorption Spectroscopy (XAS). The technique probes the fine structure that can be observed in the X-ray absorption spectra near an absorption edge. XAS can be subdivided in two regions. The first region, close (5-50 eV) to the absorption edge is called NEXAFS or XANES, both acronyms implying X-ray Absorption Near Edge Structure. This is the region where information about valence and the coordination of the probe atom can be found. Beyond this energy region (i.e. > 50 eV) one generally speaks of X-ray Absorption Fine Structure (EXAFS). The information that can be obtained from this regime concerns atomic pair distribution function. The experimental requirements for both techniques are very similar and it is beyond the scope of this manuscript to detail the differences (19). XAS has in the past been successfully combined with WAXS (20, 21) but the combination with SAXS, which adds an extra length scale, is relatively new (22, 23).

XAS is a spectroscopic technique where the transmission of a sample has to be measured as function of photon energy which is varied over the absorption edge of a probe-atom (24) This in practice means that there is a conflicting requirement with carrying out X-ray scattering methods simultaneously since this requires in general constant photon energy. This situation can be remedied by performing the experiments quasi simultaneous in which the XAS data is obtained during an energy scan and the scattering data in a brief interlude between the XAS scans. See figure 1.

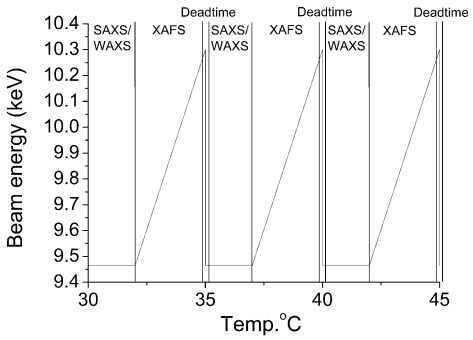

Figure 1 Data acquisition scheme for quasi- simultaneous SAXS/WAXS/XAS experiments. The horizontal scale represents the sample parameter that is varied, in this example the temperature.

The time-resolution that can be achieved in this way is dominated by the time required to carry out an energy scan since the data acquisition time of X-ray scattering can be limited to 1-5 seconds. This can be a function of the mechanics of the monochromator or of the counting statistics required to obtain an acceptable data quality. With a conventional X-ray monochromator the mechanical limitations will impose a lower limit of about 30-60 seconds/frame. Faster speeds can be achieved with special monochromators(25). This scanning technique is conventionally named QuXAFS and should not be mistaken with the energy dispersive variety of XAS where a polychromatic beam is used and the time resolution can be reduced to milliseconds (26, 27) at the expense of a reduced energy resolution and therefore lower XAS data quality.

In materials science there is a multitude of experimental problems where millisecond time-resolution is not required but where the time scale of structural developments can be tuned by choosing parameters like temperature or chemical concentration. One can think about for instance thermally induced crystallization processes or catalytic reactions. It is for these type of experiments

that we have developed the combined SAXS/WAXS/XAS equipment (23). Here we will discuss some results and limitations of the technique.

2. Results

2.1. Instrumentation

A technical drawing of the combined SAXS/WAXS/XAFS set-up is shown in figure 2. For a full technical description one is referred to our earlier work (23).

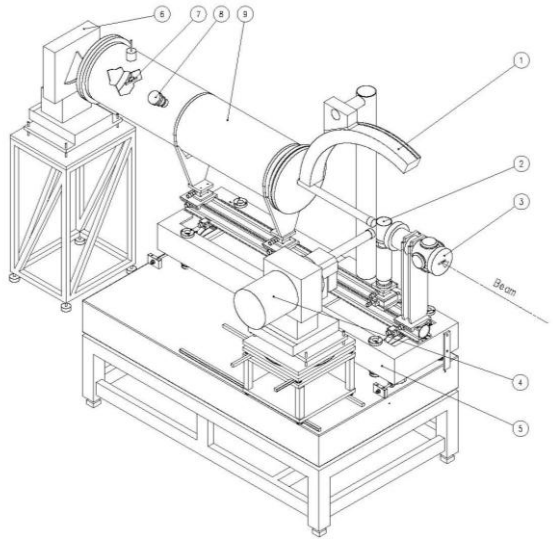

Figure 2 Technical drawing of the combined SAXS/WAXS/EXAFS set up on beam line BM26A at the European Synchrotron Radiation Source. 1- position sensitive INEL detector, 2 – sample position, 3 – intensity monitor for incoming beam, 4 – fluorescence EXAFS detector, 5 – height adjustable optical bench, 6 – position sensitive SAXS detector, 7 – Beam stop and transmitted intensity monitor, 8 – evacuation port, 9 – SAXS flight tube. (reprinted from (23))

The DUBBLE BM26A beam line receives dipole radiation of an ESRF 0.4 Tesla bending magnet. The lower energy limit is determined by the absorption of some Be windows in the beam line and is about 4 keV which means that Ti is the element from which one can still comfortably obtain XAS data. The higher energy range is limited by the mechanics of the monochromator and is around 42 keV, i.e. the Ce K-edge.

At present not sufficient experiments have been carried out to provide a detailed analysis of what time resolution is achievable for which elemental absorption edge. However, the rate limiting step is the collection of the XAS data. In the case that one only wants to collect XANES data, i.e. over a relative small energy range, a time resolution of 30-60 seconds is required for the energy scan and data collection. When the energy has to be scanned over the larger range required for EXAFS this will increase considerably.

For photon energies up to 20 keV it is still feasible to resolve SAXS diffraction distances pertaining to real space structures of around 40 nm. For lower energies this can be increased to about 80 nm.

2.2. Nanoparticle synthesis

An example where both SAXS as well as XANES/EXAFS data were required to shed light onto a formation process and chemical state of samples can be found in the formation of Co-nanostructured particles. Co nanoparticles have been formed by mixing Cobalt bis(2-ethylhexyl)sulfosuccinate, $Co(AOT)_2$, reverse micelles dispersion in n-heptane together with 1 wt% in ethanol sodium borohydride solution, according to the reaction

$$Co(AOT)_2 + 2NaBH_4 \rightarrow Co + 2NaAOT + B_2H_6 + H_2$$

.In this case the high fluidity of this solution of a reversed micellar solution was used not only for the formation of the 2-6 nm sized nanoparticles but also for directing the shape of nanoparticle superstructures. The size is generally reckoned to be a function of the amount of reducing agent added to the solution but the shape can be influenced by the water content since one can tune the microstructure from the micelles from cylindrical to spherical by varying the concentration. These nanoparticles can then either remain in solution with a surrounding protective layer or, in case of existing attractive potentials, can start to form elongated nanostructures.

The nanoparticle size is well suited for SAXS investigations but due to the small size it is very hard to obtain any diffraction information. The Scherrer broadening from which the diffraction peaks suffer, assuming that the order is already high enough to create diffraction, will be so much that it will be difficult to detect above the background due to the scattering of other components of the sample. The internal structure of these nanoparticles 'building blocks' as well as the nanostructure created when they do have an attractive potential, can be studied with X-ray absorption techniques. In figure 3 the SAXS data for three samples with identical composition but obtained by different treatment routes are shown: A) Co nanoparticles separated from the reacting mixture immediately after complete Co(II) reduction; B) Co nanoparticles formed after complete Co(II) reduction and aged in the same reacting mixture for 1 day; C) Co nanoparticles of sample A aged at room temperature in air for about one day. From these data it could be derived that self-assembled elongated microstructure (q^{-1} slope) was formed using preparation methods A and C (28). The average Co nanoclusters size was 1nm. For sample B, aging of Co nanoparticles in reaction mixture produces increase of the size of the Co nanoparticles and a mixture of clusters of 10nm and 21nm average radii was found via SAXS data modeling (28).

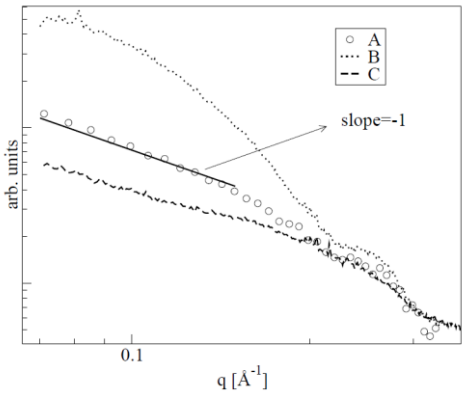

Figure 3 SAXS data of AOT reverse micellar solutions with Co-nanoparticles of three samples with identical composition but with different preparation methods. (reprinted with permission from (28))

The corresponding EXAFS spectra are shown in figure 4. From these spectra the parameters regarding the Co-Co interaction can be derived. We again observe rather different results depending on the sample processing pathway. For sample 'B' the lowest coordination number and shortest Co-Co distance of all three samples is found. In contrast the disorder, i.e. deviation from the bulk crystalline lattice is highest.

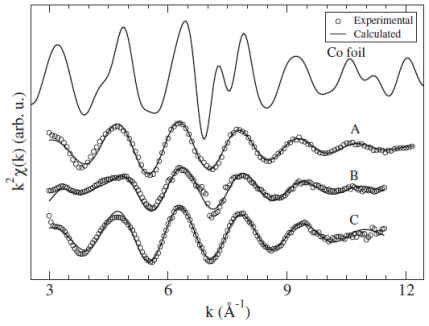

Figure 4 k-weighted EXAFS spectra of the same samples corresponding to the SAXS patterns shown in figure 3. (reprinted with permission from (28)

On the basis of the combined SAXS and EXAFS results one can derive a model for the micro- and nanostructure found in this sample. The schematic drawing for samples prepared according to the 'A' and 'C' recipes is shown in figure 4. The disordered Co nanoparticles are enclosed in cylindrical vesicles and form an elongated loose necklace. The average cluster diameter was found close to 1-2nm. Using the 'B' procedure, the microstructure is mainly unchanged, but a significant fraction of nanoparticles has a larger diameter, close to 4nm.

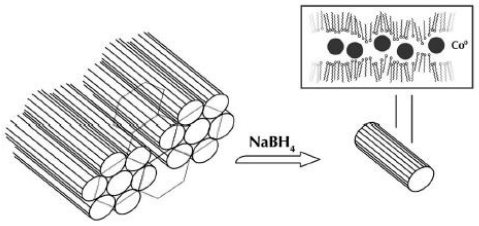

Figure 5 Schematic drawing of the nano- and microstructure of reversed micellar solutions with Co-nanoparticles obtained with the sample preparation method 'B' (as described in the text) (reprinted with permission from (28)

2.3. Inorganic catalytic systems

A second example in which the combination of SAXS/WAXS and EXAFS played a role in elucidating the growth process can be found in the study of the formation of inorganic microporous crystalline materials which can for instance be used as catalyst carriers. Here structure formation has to be studied at a very broad range of length scales. The very smallest scale is at the molecular level where the local coordination can be studied by spectroscopy. The nano scale (primary building elements) can be studied with both spectroscopy as well as diffraction and the longer range order, i. e. the crystallite formation is typically a length scale that falls in the remit of SAXS.

The specific material studied in this example is zinc-substituted microporous aluminophosphate used for the creation of molecular sieves. The starting material was a gel which was heated during the experiment and thus inducing structure formation. The initial state is amorphous, as derived from the absence of diffraction peaks in the WAXS spectrum. See figure 6a. However, at elevated temperatures the materials start to crystallize as evidenced by the occurrence of diffraction peaks. The XAFS (both XANES and EXAFS) data allow us to follow the changes in Zn^{2+} coordination number during the crystallisation process and this changes considerably during the crystallisation process when the Zn is incorporated in the crystalline fraction. See figure 6b. The interesting point to note is that we find clear changes in both the EXAFS as well as the diffraction curves but a SAXS pattern that is only slightly changing which indicates the presence of domain sizes of about 12 nm. See figure 6c. This is rather peculiar since one would expect to see at least some changes due to the fact that crystallisation is rarely such a benign event that no changes occur. A possible cause for this could be that the Zn^{2+} ions responsible for 'inducing' the formation of a particular microporous phase only comprise 2.5 wt% and therefore most of the material in the reaction gel remains amorphous/uncrystallised(29).

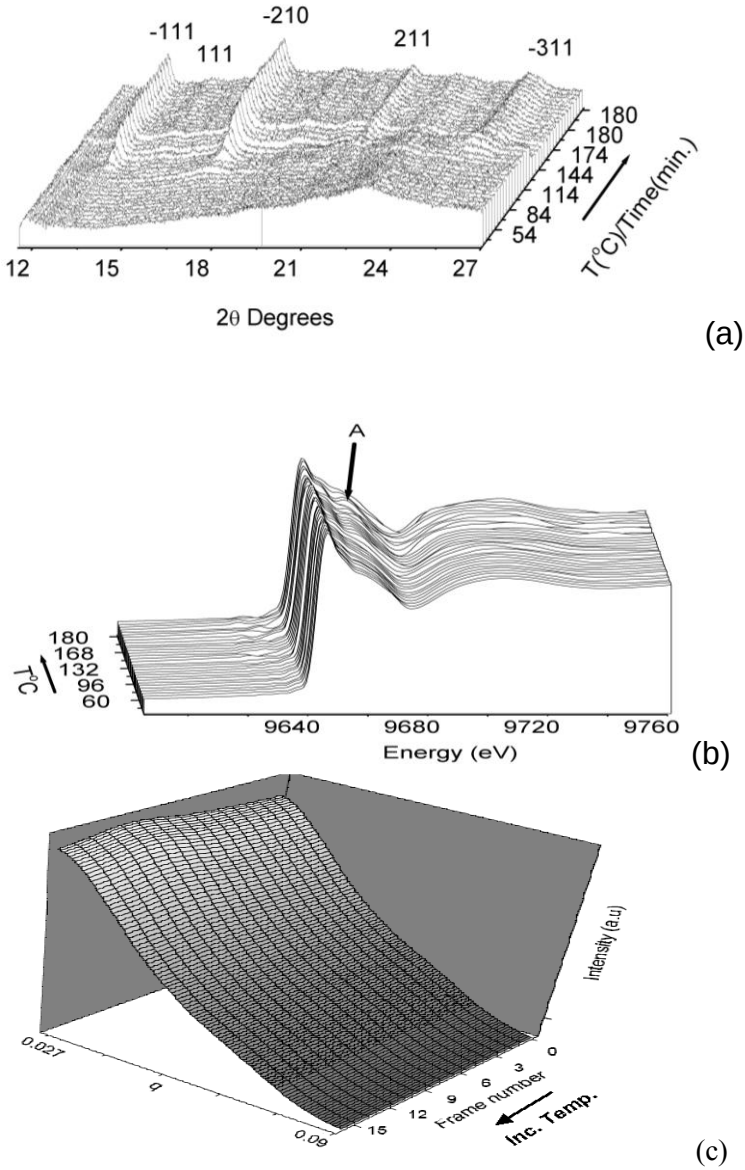

Figure 6a Time-resolved WAXS patterns from a crystallising gel. 6b- corresponding X-ray spectroscopy patterns, 6c corresponding SAXS patterns. The figures do have different orientations for clarity. Reprinted with permission from (22)

However, some clarity in the situation can be obtained when we consider one of the parameters that is most sensitive to changes, i.e. the invariant.

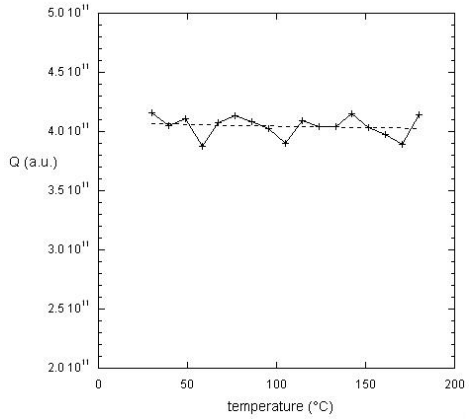

Figure 7 Time development of the invariant, Q, for the scattering experiment described above and in figure 6. (reprinted from (23))

For a two phase system the invariant can be given by: $Q = \int I(\vec{q})dV = \int_{q=0}^{q=\infty} I(q)q^2 dq = \left\langle n_e \right\rangle^2 \phi_1 \phi_2$ in which $\left\langle n_e \right\rangle^2$ is the electron density contrast between the two phases and $\phi_{i,j}$ the volume fractions of the two phases. In figure 7 the time development of the invariant is sketched and one finds that within the experimental error margin *Q* remains unchanged. Since we do know from the SAXS data that the domain size also remains unchanged the only logical conclusion, apart from a non functioning detector, as was mentioned previously, is that in the phase separated system one of the phases crystallizes whilst the other remains amorphous. This process takes place without material transport between the two phases and with no appreciable changes in density of the crystallizing phase. As was mentioned in the introduction it is often rather difficult to prove the absence of any change and therefore the proper functioning of the detector was checked.

3. Limitations

The system that we have developed is unfortunately not universally applicable. In this section we will discuss some of the limitations.

The energy range over which this type of technique combination can be applied is limited. Obviously one would like to perform the diffraction and scattering experiments close to the energy imposed by the XAS experiment. For WAXS or powder diffraction this is in general possible provided that there is a position sensitive detector available that can operate at this energy and has the required spatial resolution. For gas filled detectors, like the Inel (30), the photon detection efficiency is rather low when the photon energy exceeds 15 keV. The low count rate capability of this type of detector is in general not a major problem thanks to the limited time resolution for which the combined set-up has been developed. However, if this is combined with a low efficiency then this becomes a major problem and different detectors have to be used. This can be CCD based systems but these will suffer from a smaller accessible q-range. Also at higher energies the diffraction pattern will be compressed and one might loose too much resolution in which case one has to revert to a diffractometer style of data acquisition which will increase the time required to obtain a data frame.

Similar arguments can be given for the SAXS detector with the obvious caveat that a real photon counting detector would be the best choice which unfortunately rules out a large number of CCD

detectors. A second effect of an increase in photon energy is a loss in low angle resolution. The parasitic scatter cone of a beam line is determined by the slit settings and the beam size. Since this is unlikely to change much as function of energy but the scattering patterns get compressed this means that the real low angle part of the scattering pattern will disappear in the parasitic scattering cone. This effect can partially be overcome by using a micro focus beam but this has as a down side that the possibility that radiation damage can occur in the small exposed volume increases.

An alternative solution would be to accept that the energies at which the different data sets have to be taken are further removed from each other. This solution is less favourable due to the longer energy scanning time required. This will most likely also require an adjustment, not only in the monochromator settings, but also in those of the other optical components of the beam line. In theory this can be achieved by storing these positions in a look-up table but this is only a theoretical option and in practice either the XAS or the SAXS data quality will suffer a loss in quality although with the newer generation of monochromators these limitations have become less important.

A limitation that exists in the case of the EXAFS experiments is that the doping with the probe atom should be high enough in order to generate sufficient statistics. The maximum length of the energy scan required to obtain the EXAFS results is dictated by the time scale on which structural developments take place. If this is too short then obviously it will be impossible to obtain relevant data. An example where the application of the technique failed was in the case of temperature induced cordierite glass ($Mg_2Al_4Si_5O_{18}$) crystallisation which was doped a crystallisation enhancer in the form of 0.34 mol% Cr_2O_3 (31). This system would be an ideal candidate for investigations with three techniques. Already an extensive study has been made with a combined SAXS and WAXS experiment. However, the Cr doping was found too low to be able the elucidate the role of this atom in the initial stages of crystallisation when the required time-resolution was on the order of 1 minute/frame. Increasing the X-ray intensity to counteract this requires also detectors that can handle the increased count rate but also the sample has to be able to withstand this flux for an extended period. With modern beam lines, even for inorganic samples, this is not always the case (32).

4. Conclusions

We have constructed a combined SAXS/WAXS/EXAFS set up which can for certain classes of samples generate data sets in which the fact that the data is obtained simultaneously allows the elucidation of the different steps in growth processes ranging from the molecular scale to long range structural features. Under favourable conditions time resolutions of 1 minute/frame can be achieved which is compatible with numerous experiments in for instance inorganic synthesis of micro-structured materials.

The applied technique is useable for samples where the EXAFS edges are not too far removed from the energy range where SAXS data can be obtained. Also limitations exist when there are low concentrations of the probe atom in the sample. However, in the cases that the combination of these three technique can be applied it generates a wealth of information which is difficult to surpass by other means.

5. Acknowledgements

The data and figures on the AOT Co-nanoparticle synthesis were graciously provided by Dr. A. Longo. The DUBBLE staff are acknowledged for technical support. NWO/FWO is thanked for granting the beam time on BM26A. Piet Lassing is thanked for the technical drawings.

Figures 3, 4 and 5 have been reprinted with permission from A. Longo et al. Journal of Applied Physics 105, 114308, Copyright 2009, American Institute of Physics. Figure 6 has been reprinted with permission from A. Beale et al. Journal American Chemical Society 128, 2006, 12386

6. References

1. Russell, T. P., and J. T. Koberstein. 1985. Simultaneous Differential Scanning Calorimetry And Small-Angle X-Ray-Scattering. Journal Of Polymer Science Part B-Polymer Physics 23:1109-1115.
2. Bark, M., H. G. Zachmann, R. Alamo, and L. Mandelkern. 1992. Investigations Of The Crystallization Of Polyethylene By Means Of Simultaneous Small-Angle And Wide-Angle X-Ray-Scattering. Makromolekulare Chemie-Macromolecular Chemistry And Physics 193:2363-2377.
3. Bras, W., G. E. Derbyshire, A. J. Ryan, G. R. Mant, A. Felton, R. A. Lewis, C. J. Hall, and G. N. Greaves. 1993. Simultaneous Time Resolved Saxs and Waxs Experiments Using Synchrotron Radiation. Nuclear Instruments & Methods in Physics Research Section a-Accelerators Spectrometers Detectors and Associated Equipment 326:587-591.
4. Fernandez-Ballester, L., T. Gough, F. Meneau, W. Bras, F. Ania, J. C. Francisco, and J. A. Kornfield. 2008. Simultaneous birefringence, small- and wide-angle X-ray scattering to detect precursors and characterize morphology development during flow-induced crystallization of polymers. Journal Of Synchrotron Radiation 15:185-190.
5. Bryant, G. K., H. F. Gleeson, A. J. Ryan, J. P. A. Fairclough, D. Bogg, J. G. P. Goossens, and W. Bras. 1998. Raman spectroscopy combined with small angle x-ray scattering and wide angle x-ray scattering as a tool for the study of phase transitions in polymers. Review of Scientific Instruments 69:2114-2117.
6. Rastogi, S., J. G. P. Goossens, and P. J. Lemstra. 1998. An in situ SAXS/WAXS/Raman spectroscopy study on the phase behavior of syndiotactic polystyrene (sPS)/solvent systems: Compound formation and solvent (dis)ordering. Macromolecules 31:2983-2998.
7. Bras, W., G. E. Derbyshire, D. Bogg, J. Cooke, M. J. Elwell, B. U. Komanschek, S. Naylor, and A. J. Ryan. 1995. Simultaneous Studies of Reaction-Kinetics and Structure Development in Polymer Processing. Science 267:996-999.
8. Wurm, A., R. Soliman, J. G. P. Goossens, W. Bras, and C. Schick. 2005. Evidence of pre-crystalline-order in super-cooled polymer melts revealed from simultaneous dielectric spectroscopy and SAXS. Journal of Non-Crystalline Solids 351:2773-2779.
9. Ezquerra, T. A., I. Sics, A. Nogales, Z. Denchev, and F. J. Balta-Calleja. 2002. Simultaneous crystalline-amorphous phase evolution during crystallization of polymer systems. Europhysics Letters 59:417-422.
10. Mesu, J. G., A. M. Beale, F. M. F. de Groot, and B. M. Weckhuysen. 2006. Probing the influence of X-rays on aqueous copper solutions using time-resolved in situ combined video/X-ray absorption near-edge/ultraviolet-visible spectroscopy. Journal Of Physical Chemistry B 110:17671-17677.
11. Terrill, N. J., P. A. Fairclough, E. Towns-Andrews, B. U. Komanschek, R. J. Young, and A. J. Ryan. 1998. Density fluctuations: the nucleation event in isotactic polypropylene crystallization. Polymer 39:2381-2385.
12. Chu, B., and B. S. Hsiao. 2001. Small-angle X-ray scattering of polymers. Chemical Reviews 101:1727-1761.

13. Wang, Z. G., B. S. Hsiao, E. B. Sirota, and S. Srinivas. 2000. A simultaneous small- and wide-angle X-ray scattering study of the early stages of melt crystallization in polyethylene. Polymer 41:8825-8832.
14. Strobl, G. 2000. From the melt via mesomorphic and granular crystalline layers to lamellar crystallites: A major route followed in polymer crystallization? Eur. Phys. J. E 3:165-183.
15. Bras, W., I. P. Dolbnya, D. Detollenaere, R. van Tol, M. Malfois, G. N. Greaves, A. J. Ryan, and E. Heeley. 2003. Recent experiments on a combined small-angle/wide-angle X-ray scattering beam line at the ESRF. Journal of Applied Crystallography 36:791-794.
16. Gilbert, B. 2008. Finite size effects on the real-space pair distribution function of nanoparticles. Journal of Applied Crystallography 41:554-562.
17. Chupas, P. J., K. W. Chapman, G. Jennings, P. L. Lee, and C. P. Grey. 2007. Watching nanoparticles grow: The mechanism and kinetics for the formation of TiO2-supported platinum nanoparticles. Journal of the American Chemical Society 129:13822-+.
18. Michel, F. M., L. Ehm, S. M. Antao, P. L. Lee, P. J. Chupas, G. Liu, D. R. Strongin, M. A. A. Schoonen, B. L. Phillips, and J. B. Parise. 2007. The structure of ferrihydrite, a nanocrystalline material. Science 316:1726-1729.
19. Koningsberger, D. C., and P. R., editors. 1988. X-Ray Absorption. Wiley.
20. Dent, A. J., M. Oversluizen, G. N. Greaves, M. A. Roberts, G. Sankar, C. R. A. Catlow, and J. M. Thomas. 1995. A Furnace Design for Use in Combined X-Ray-Absorption and Diffraction up to a Temperature of 1200-Degrees-C - Study of Cordierite Ceramic Formation Using Fluorescence Qexafs/Xrd. Physica B 209:253-255.
21. Sankar, G., P. A. Wright, S. Natarajan, J. M. Thomas, G. N. Greaves, A. J. Dent, B. R. Dobson, C. A. Ramsdale, and R. H. Jones. 1993. Combined Quexafs-Xrd - a New Technique in High-Temperature Materials Chemistry - an Illustrative in-Situ Study of the Zinc Oxide-Enhanced Solid-State Production of Cordierite from a Precursor Zeolite. Journal of Physical Chemistry 97:9550-9554.
22. Beale, A. M., A. M. J. van der Eerden, S. D. M. Jacques, O. Leynaud, M. G. O'Brien, F. Meneau, S. Nikitenko, W. Bras, and B. M. Weckhuysen. 2006. A combined SAXS/WAXS/XAFS setup capable of observing concurrent changes across the nano-to-micrometer size range in inorganic solid crystallization processes. Journal Of The American Chemical Society 128:12386-12387.
23. Nikitenko, S., A. M. Beale, A. M. J. van der Eerden, S. D. M. Jacques, O. Leynaud, M. G. O'Brien, D. Detollenaere, R. Kaptein, B. M. Weckhuysen, and W. Bras. 2008. Implementation of a combined SAXS/WAXS/QEXAFS set-up for time-resolved in situ experiments. Journal Of Synchrotron Radiation 15:632-640.
24. D. C. Koningsberger, D. C., and R. Prins, editors. 1988. X-Ray Absorption. Wiley.
25. Frahm, R., M. Richwin, and D. Lutzenkirchen-Hecht. 2005. Recent advances and new applications of time-resolved X-ray absorption spectroscopy. Physica Scripta T115:974-976.
26. Dent, A. J. 2002. Development of time-resolved XAFS instrumentation for quick EXAFS and energy-dispersive EXAFS measurements on catalyst systems. Topics in Catalysis 18:27-35.
27. Newton, M. A., B. Jyoti, A. J. Dent, S. G. Fiddy, and J. Evans. 2004. Synchronous, time resolved, diffuse reflectance FT-IR, energy dispersive EXAFS (EDE) and mass spectrometric investigation of the behaviour of Rh catalysts during NO reduction by CO. Chemical Communications:2382-2383.
28. Longo, A., F. Giordano, F. Giannici, A. Martorana, G. Portale, A. Ruggirello, and V. T. Liveri. 2009. Combined small-angle x-ray scattering/extended x-ray absorption fine structure study of coated Co nanoclusters in bis(2-ethylhexyl)sulfosuccinate. Journal of Applied Physics 105.
29. O'Brien, M. G., A. M. Beale, C. R. A. Catlow, and B. M. Weckhuysen. 2006. Unique organic-inorganic interactions leading to a structure-directed microporous aluminophosphate

crystallization as observed with in situ Raman spectroscopy. Journal of the American Chemical Society 128:11744-11745.

30. Evain, M., P. Deniard, A. Jouanneaux, and R. Brec. 1993. POTENTIAL OF THE INEL X-RAY POSITION-SENSITIVE DETECTOR - A GENERAL STUDY OF THE DEBYE-SCHERRER SETTING. Journal of Applied Crystallography 26:563-569.
31. Bras, W., S. M. Clark, G. N. Greaves, M. Kunz, W. van Beek, and V. Radmilovic. 2009. Nanocrystal Growth in Cordierite Glass Ceramics Studied with X-ray Scattering. Crystal Growth & Design 9:1297-1305.
32. Mesu, J. G., A. M. J. van der Eerden, F. M. F. de Groot, and B. M. Weckhuysen. 2005. Synchrotron radiation effects on catalytic systems as probed with a combined in-situ UV-Vis/XAFS spectroscopic setup. Journal Of Physical Chemistry B 109:4042-4047.